

Interface induced perpendicular magnetic anisotropy in Co/CoO/Co thin film structure: An in-situ MOKE investigation

Dileep Kumar,^{1, a)} Ajay Gupta,¹ P. Patidar,² K.K. Pandey,³ T. Sant,³ and S.M Sharma³

¹⁾ *UGC-DAE Consortium for Scientific Research, Khandwa Road, Indore-452017, India*

²⁾ *School of Nanotechnology, RGPV, Bhopal-462021*

³⁾ *High Pressure and synchrotron radiation physics division, BARC, Trombay, Mumbai- 400 085*

(Dated: 21 August 2012)

Co /CoO/Co polycrystalline film was grown on Si (001) substrate and magnetic properties have been investigated using *in-situ* magneto-optic Kerr effect during growth of the sample. Magnetic anisotropy with easy axis perpendicular to the film surface has been observed in top Co layer, whereas bottom layer was found to be soft with in-plane magnetization without any influence of top layer. Ex-situ in-plane and out-of-plane diffraction measurements revealed that the growth of Co on oxidized interface takes place with preferential orientation of c-axis perpendicular to the film plane, which results in the observed perpendicular magnetic anisotropy. Texturing of the c-axis is expected to be a result of minimization of the interface energy due to hybridization between Co and oxygen at the interface.

^{a)}Electronic mail: dkumar@csr.res.in

Perpendicular magnetic anisotropy (PMA) is a newly emergent area of thin film magnetism in which the preferential alignment of the spins perpendicular to the film surface plays an important role in the functioning of the spintronic devices. In the past, magnetic materials which exhibit PMA drew wide attention because of their use in perpendicular recording media.^{1,2} Recently, thin film nanostructures which exhibit strong PMA rapidly actuated extensive research efforts because of the great current interest in perpendicular spin valves (p-SVs) and magnetic tunnel junction (p-MTJs) devices.³ Strong PMA appears in periodically altered ferromagnetic (FM)/ noble metal(NM) multilayers such as Co/Pt, Co/Pd, Co/Au and CoFeB/Pd.⁴⁻⁷ In these multilayer systems, increase in the orbital momentum of Co due to the strong hybridization between the 3d orbitals of the transition metal and the 5d orbitals of heavy metals at the interface is known to be responsible for the strong PMA.^{4,6} As the hybridization is localized at the interfaces, therefore strong PMA appears only with very thin magnetic layer (typically in the range of 3 Å to 6 Å thick). Most of the PMA systems have already been used as magnetic electrodes in magnetic tunnel junctions, however because of limited thermal stability and ultra-thin magnetic layer, which substantially reduces the effective spin polarization of the electrode and leads to quite small tunnelling magneto- resistance (TMR) value, none of them are useful from application point of view.

Recently, L.E Nistor *et al.*⁸ studied Pt/Co/Oxide and Oxide/Co/Pt thin film structures and obtained strong PMA with Co layer as thick as 30 Å after annealing at 350°C. They have demonstrated that despite the degraded growth of Co on Oxide, the Oxide/Co interface brings much more PMA as compare to Pt/Co. The origin of enhanced value of PMA was attributed to the alignments of the Co-O bonds due to hybridization between Co and O orbitals at the interface. In another study by Qin-Liet *al.*⁹ a Co/ Pt bilayers with 15 Å thick Co have been prepared by incorporating some oxygen atoms at interface. A significant increase in PMA after annealing at 250°C-400°C was attributed to the formation of large number of Co-O-Pt or Pt-Co-O bonds orientated normal to the interface. In this study, it has also been demonstrated that an additional 20 Å thick Co on Co/CoO/Pt structure aligned perpendicular to the film plane due to the exchange coupling with underneath multilayer. In fact the role of oxygen to improve PMA opened up another avenue to realizing thick, thermally stable electrodes for both p-SVs and p-MTJs and therefore being studied in detail both experimentally¹⁰ and theoretically.¹¹ Although these results are quite encouraging but

still there is a lack of clear understanding in this area. In this letter, we have studied the growth of thick Co layer($\sim 100\text{\AA}$) on uniformly oxidized CoO layer which has been prepared by thermally oxidizing thick Co layer on Si (001) substrate. Magnetic properties during each step of growth of the films have been investigated using *in-situ* magneto optical Kerr effect (MOKE). In contrast to the previous studies, We have obtained significant PMA in much higher thickness of Co film even in as prepared stage (without post thermal annealing the structure). Using depth resolved in-situ MOKE, it is also demonstrated that oxide layer (CoO) of 26 \AA thickness nicely separate different magnetic state of adjacent (bottom and top) two magnetic layers.

Co/CoO/Co multilayer structure has been grown in an ultra-high vacuum chamber in the base pressure $\sim 2 \times 10^{-8}$ mbar with facility for e-beam evaporation, and MOKE measurement.¹² Film thickness was measured in-situ using a calibrated quartz crystal thickness monitor. Growth of the sample was done on silicon substrate in three steps; i) deposition of ~ 500 \AA thick Co film at room temperature (denoted as F1), ii) in-situ annealing at 450°C for 1 hour in a vacuum of $\sim 5 \times 10^{-4}$ mbar (denoted as F2) in order to form a thin oxide layer at the surface. Annealing is also expected to results in transformation of hcp phase of Co to fcc phase¹³, and iii) deposition of another ~ 100 \AA thick Co film (denoted as F3) on top of it. In-situ hysteresis loops were measured using MOKE in longitudinal geometry (L-MOKE) after each step of deposition (F1, F2 and F3). It may be noted that after the second stage, a part of the sample (F2- film) was preserved by masking. Another Co film on Si substrate was deposited separately in the identical conditions, which is expected to be identical to film F1. These films were used for ex-situ measurements.

Figure 1 gives hysteresis loops recorded in-situ after different stages F1, F2, and F3 of sample growth. Film F1 exhibits a square loop with a coercive field (H_c) of 21 ± 0.5 Oe. As shown in fig. 1(a), small variation in shape with azimuthal direction was observed, suggesting presence of a very weak in-plane uniaxial magnetic anisotropy in F1 film. In film F2 (fig. 1b), coercivity increased almost 3 times as compare to F1 film and similar loops with azimuthal direction in this figure, suggesting disappearance of weak in-plane magnetic anisotropy, which might have induced due to the stresses produced during the growth of the film F1. It is important to note that, in film F3 (fig.1c), when an additional Co layer is deposited on F2 film, coercivity remains almost the same, but it becomes difficult to saturate the hysteresis loop using a magnetic field of ~ 300 Oe, which is the maximum

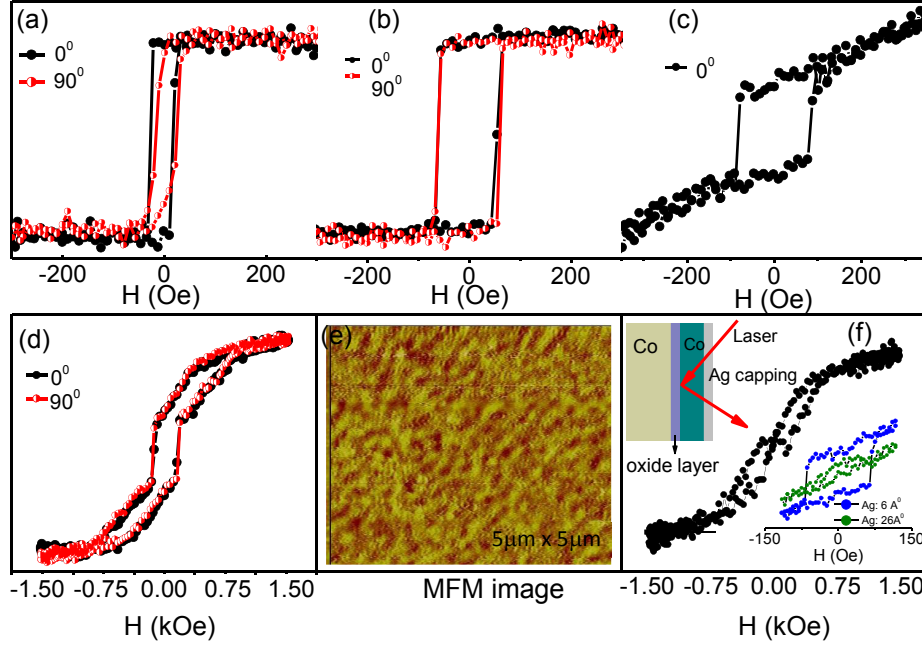


FIG. 1. (Colored online) Hysteresis loops after the different stages of the sample growth; a) F1 b) F2 and c) F3. (d) Hysteresis loop of F3-film recorded with higher magnetic field using ex-situ MOKE; $=0^\circ$, 90° angles corresponds to hysteresis loop along easy direction and hard direction of magnetization. (e) MFM image of the F3 film (f) loop after 26 Å thick Ag layer on top of F3 film. In set of the figure shows two representative loops, recorded in-situ with 6 Å and 26 Å thick capping layer

field which could be applied in our in-situ set-up. Hysteresis loop of the F3-film was also measured ex-situ under higher applied magnetic field and is given in fig.1(d). It may be noted that the hysteresis loop is still not getting saturated upto 1500Oe. No variation in the hysteresis loops was observed as a function of azimuthal angle. This indicates presence of a strong perpendicular magnetic anisotropy in F3 film. Magnetic force microscopy (MFM) image in figure 1(e), with dense stripe magnetic domain structure, strongly confirms the perpendicular magnetization in this film.

It is necessary to mention here that He-Ne laser of wavelength $=6328\text{Å}$ is used for MOKE measurements, which penetrates typically upto 200 to 300 Å in depth of Co film.¹⁴ Therefore, double hysteresis loop of F3 film may contain combined hysteresis loop of both bottom and top Co layers. In order to confirm this, a small piece of F3 film was reloaded into the chamber and an Ag film was deposited on it. Hysteresis loops were recorded simultaneously

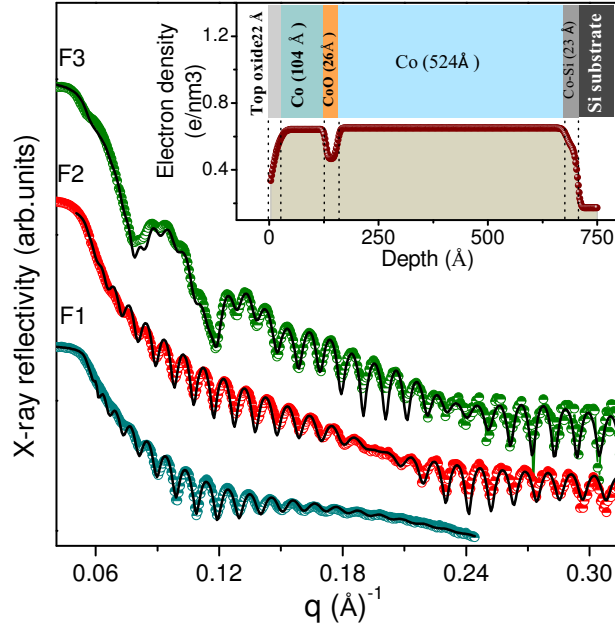


FIG. 2. (Colored online), i) Experimental (dotted symbol) and fitted (line) x-ray reflectivity patterns of F1, F2 and F3 films. Inset gives electron density (ρ) profile and final structure of the sample F3 film. In order to elucidate the origin of the observed magnetic properties and to correlate the same with structure of the sample, x-ray reflectivity and x-ray diffraction measurements were done on these films

as a function of the thickness of nonmagnetic Ag capping layer. This provides hysteresis loops from decreasing depth of the film because of the laser penetration into the Co film is limited by the top Ag layer. These measurements reveal that the soft loop in middle gradually disappears and hard loop remains in place after 26Å thick Ag layer on top. Hysteresis loop with 26Å thick capping layer was also recorded using ex-situ MOKE with higher magnetic field and is shown in figure 1(f). Decreased contribution of the soft (center loop) part with increasing thickness of Ag reveals that the bottom Co remains soft with in-plane magnetic moments whereas the top Co layer, which was deposited on F2 film, possesses perpendicular magnetic anisotropy.

Figure 2 gives x-ray reflectivity patterns together with best fit to the data using Parratt's formalism.¹⁵ Electron density depth profile of sample F3 as shown in inset of the figure 2, strongly confirms the formation of 26Å thick oxide layer with electron density 28% less than that of bulk Co. In fact, this sample also displays exchange bias, after being field cooled to 10K, supporting the formation of native antiferromagnetic oxide layer of CoO. It may be

noted that the interfaces at both side of oxide layer are found relatively sharp ($\sigma_{\text{Co-on-CoO}} = 4.1\text{\AA}$ and $\sigma_{\text{CoO-on-Co}} = 5.2\text{\AA}$) and are comparable to the substrate roughness, which indicates a homogeneous thermal oxidation of the bottom Co layer.⁸

Recently H.X tang *et al.*¹¹ investigated origin of PMA at the interface between ferromagnetic transition metals and metallic oxides via first principles theoretical calculation. Origin of strong PMA due to the interfacial oxide in Fe/ MgO(100) structure was attributed to the hybridization between Fe-3d and O-2p orbitals. Experimentally, in the Pt/Co/AlOx trilayer system, it has been observed that a substantial amount of oxygen at the interface induced strong PMA in this system due to Co and O atomic hybridization at the interface.¹⁰ Hybridization results Co-O orbitals perpendicular to the interface due to minimization of Co-O binding energy and leads to a strong PMA in this trilayer system. A similar effect has also been observed in other systems such as CoO/[Co/Pt], Co/native oxide/Pt and Pt/Co/Oxide etc.^{8,9} It is important to note that hybridization is localized at the interfaces and therefore, even with oxygen mediated interfaces (as mentioned above), significant PMA is observed only in ultra thin magnetic layer ranging from few \AA to a few tens of \AA .^{8,9} In the present work, PMA in 104 \AA thick Co layer is some what surprising and can not be understood only in-terms of interface hybridization.

In order to explore the origin of the PMA in top Co layer, structure of the films was investigated using energy dispersive x-ray diffraction (EDXRD) at BM-11 beamline of Indus-2, synchrotron radiation source, Indore which is a white x-ray beamline.¹⁶ In order to find in-plane and out-of-plane structure of sample F3, measurements were carried out in two geometries as shown in inset of the fig.3; i) grazing incidence out of plane (OP-XRD) geometry, where the incident beam falls at very low grazing angle ($\theta_{in} \sim 0.05^\circ$) on the sample which was kept vertically, while the detector was fixed at $2\theta_{out} \sim 20^\circ$ in the horizontal direction. In this case the scattering vector q lies $\sim 10^\circ$ to the film normal and, therefore, information is obtained about the scattering planes almost parallel to the film surface. ii) Grazing incidence in-plane (IP-XRD) geometry, where both incident and diffracted beam make an angle of 0.05° in vertical direction and detector was fixed at $\sim 20^\circ$ in the plane of the film. In this case scattering vector lies almost in the film plane and therefore, information is obtained about the scattering planes perpendicular to the film surface, which was kept horizontal.

The OP-XRD pattern of the F1 film exhibits three broad overlapping peaks, which corresponds to (101), (002) and (100) planes of hcp Co. In addition a faint peak around 3.56 \AA

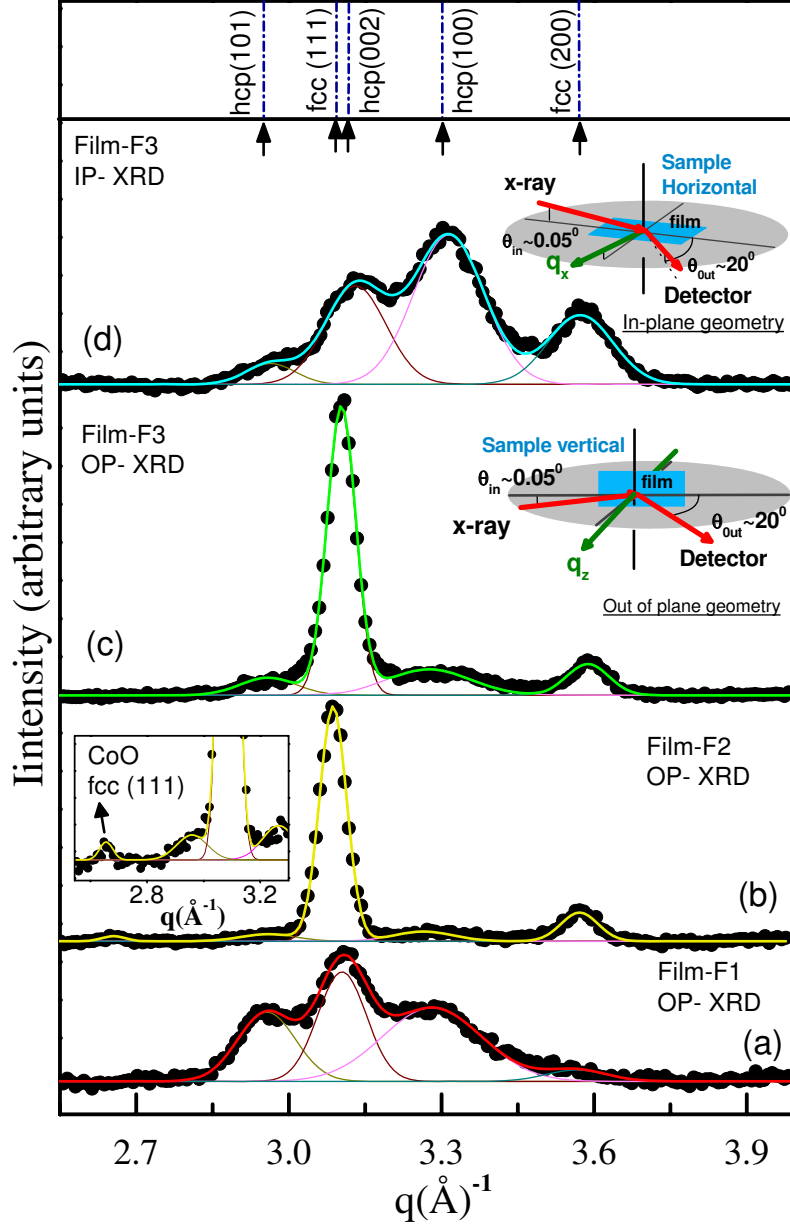


FIG. 3. (Colored online) Fitted XRD patterns in out of plane geometry (OP-XRD) a) for F1, b) for F2 and c) for F3 sample. d) fitted in-plane XRD (IP-XRD) for F3 sample. All samples measured at 0.05° incident angle. Geometries used for the measurements are given in in-set of the figure

is also visible which corresponds to (200) reflection of fcc phase. Further, (111) reflection of fcc phase at $q \sim 3.08 \text{ \AA}^{-1}$ is very close to (002) reflection of hcp phase at $q \sim 3.10 \text{ \AA}^{-1}$ and the two cannot be differentiated because of the large width of the peaks. Thus the film F1 consist of mainly hcp phase with small content of fcc phase. After thermal annealing (film

TABLE I. . Results of fitting of XRD patterns taken in in-plane (IP) and out of plane (OP) geometry for sample F3; typical error bars, as obtained from the least square fitting of the XRD data approx. $\pm 2\%$ in the value of normalized area, I_A .

	q	I_A	hkl	Co-phase
Geometry	(\AA^{-1})	(%)		
OP-XRD	2.59	08	101	hcp
	3.11	64	111+002	fcc+hcp
	3.28	17	100	hcp
	3.58	11	200	fcc
IP-XRD	2.96	04	101	hcp
	3.12	27	111+002	fcc+hcp
	3.30	49	100	hcp
	3.57	20	200	fcc

F2) diffraction pattern gets changed significantly; The peaks around $q=3.087\text{\AA}$ and $q=3.56\text{\AA}$ become prominent, while the intensity of the hcp (100) and hcp (101) peaks at $q \sim 3.016\text{\AA}$ and $q \sim 3.271\text{\AA}$ get reduced significantly. Thus thermal annealing results in transformation of hcp phase of Co to fcc phase. This is in agreement with earlier studies where thermal annealing above 350°C results in formation of fcc phase.^{13,17} In film F3, the relative intensities of hcp (100) and hcp (101) peaks at $q \sim 3.016\text{\AA}$ and $q \sim 3.271\text{\AA}$ again shows an increase. Further the position of the peak at $q \sim 3.087\text{\AA}$ shows a shift towards higher q , suggesting that the peak now has a higher contribution of hcp (002) reflection. Thus the Co film deposited on oxide layer is predominantly in hcp phase. Figure 3(d) shows the IP- XRD of film F3. A comparison of IP-XRD and OP-XRD of film F3 in table-I clearly shows that the intensity (I_A) of hcp (002) peak is substantially lower in the IP-XRD as compared to that in the OP-XRD. This suggest that c-axis of top hcp-Co layer is preferentially oriented out-of-plane.

It may be noted that the hexagonal Co possesses an inherent uniaxial magnetic anisotropy with c-axis being the easy magnetization direction.¹⁸ Therefore, in the present case textured growth of top Co layer on CoO layer leads to a volume contributed perpendicular magnetic anisotropy. The possible cause of the textured growth of hcp-Co on oxide surface can be

as follows. During the initial stages of Co deposition hybridization between Co and O at the interface leads to set Co-O bonds perpendicular to the interface.⁸⁻¹¹ Perpendicular Co orbital moment at the interface would help to grow hcp-Co with c-axis aligned preferentially perpendicular to the film surface due to a significant lowering of the anisotropy energy.⁴ A similar effect has been predicted by H. Ouyang *et al.*¹⁹ through electronic structure calculations in case of Co/Pt multilayer where interface hybridization was tailored by preferred orientation of a NiO buffer layer.

In conclusion, the growth behavior of Co thin film on CoO surface has been studied *in-situ* using MOKE. A clear perpendicular magnetic anisotropy with easy axis perpendicular to the Co-CoO interface has been observed in 104Å thick Co film. This is in contrast to the earlier studies, where PMA has been observed only in ultra thin film of thickness $\sim 25\text{\AA}$. Thus in present case one is able to obtain PMA even in film thickness with an order of magnitude higher. The origin of PMA in film is attributed to the textured growth of hcp Co with c-axis perpendicular to the film surface. Using depth resolved MOKE; it has been unambiguously shown that only top Co layer possess PMA, whereas bottom layer was found to be soft with in-plane magnetization without any influence of top layer. It is important to mention that most of the insulating layers used in TMR structures are metal oxide layers, therefore it could be possible to deposit thick magnetic electrode, which may lead to increased effective spin polarization and hence TMR value.

REFERENCES

- ¹C. W. Chen, J. Mater. Sci. **26**, 1705 (1991).
- ²S. Mangin, D. Ravelosona, J. A. Katine, M. J. Carey, B. D. Terris, and E. E. Fullerton, Nature Mat. **5**, 210 (2006).
- ³S. Ikeda, K. Miura, H. Yamamoto, K. Mizunuma, H. D. Gan, M. Endo, S. Kanai, J. Hayakawa, F. Matsukura, and H. Ohno, Nature Mat. **9**, 721 (2010).
- ⁴N. Nakajima, T. Koide, T. Shidara, H. Miyauchi, H. Fukutani, A. Fujimori, K. Iio, T. Katayama, M. Nývlt, and Y. Suzuki, Phys. Rev. Lett. **81**, 5229 (1998).
- ⁵B. Hu, N. Amos, Y. Tian, J. Butler, D. Litvinov, and S. Khizroev, J. Appl. Phys. **109**, 034314 (2011).
- ⁶D. Weller, Y. Wu, J. Stöhr, M. G. Samant, B. D. Hermsmeier, and C. Chappert, Phys.

- Rev. B **49**, 12888 (May 1994).
- ⁷F. J. A. den Broeder, D. Kuiper, A. P. van de Mosselaer, and W. Hoving, Phys. Rev. Lett. **60**, 2769 (Jun 1988).
- ⁸L. E. Nistor, B. Rodmacq, S. Auffret, and B. Dieny, Appl. Phys. Lett. **94**, 012512 (2009).
- ⁹Q.-L. Lv, J.-W. Cai, H.-Y. Pan, and B.-S. Han, Appl. Phys. Exp. **3**, 093003 (2010).
- ¹⁰B. Rodmacq, A. Manchon, C. Ducruet, S. Auffret, and B. Dieny, Phys. Rev. B **79**, 024423 (Jan 2009).
- ¹¹H. X. Yang, M. Chshiev, B. Dieny, J. H. Lee, A. Manchon, and K. H. Shin, Phys. Rev. B **84**, 054401 (Aug 2011).
- ¹²D. Kumar, S. Potdar, V. R. Reddy, and A. Gupta, J. Phys.: Conf. Ser. **114**, 012034 (2008).
- ¹³M. Jergel, I. Cheshko, Y. Halahovets, P. iffalovic, I. Matko, R. Senderk, S. Protsenko, E. Majkov, and S. Luby, J. Phys. D: Appl. Phys. **37**, 2583 (2004).
- ¹⁴K. Sarathlal, D. Kumar, V. Ganesan, and A. Gupta, Appl. Surf. Sci. **258**, 4116 (2012).
- ¹⁵L. G. Parratt, Phys. Rev. **95**, 359 (Jul 1954).
- ¹⁶K. K. Pandey, D. Kumar, A. Dwivedi, A. Gupta, and S. M. Sharma, AIP Conference Proceedings **1447**, 483 (2012).
- ¹⁷D. Kumar and A. Gupta, J. Magn. Magn Mater. **308**, 318 (2007).
- ¹⁸K. V. Sarathlal, D. Kumar, and A. Gupta, Appl. Phys. Lett. **98**, 123111 (2011).
- ¹⁹H. Ouyang, Y.-H. Han, S.-C. Lo, C.-H. Su, Y.-R. Shiu, K.-W. Lin, R. D. Desautels, and J. van Lierop, Phys. Rev. B **81**, 224412 (Jun 2010).